PLOS | ONE

RESEARCH ARTICLE

C^1 Positive Surface over Positive Scattered Data Sites

Farheen Ibraheem[1]*, Malik Zawwar Hussain[2], Akhlaq Ahmad Bhatti[1]

1 National University of Computer and Emerging Science, Lahore, Pakistan, **2** Department of Mathematics, University of the Punjab, Lahore, Pakistan

* farheen.butt@gmail.com

Abstract

The aim of this paper is to develop a local positivity preserving scheme when the data amassed from different sources is positioned at sparse points. The proposed algorithm first triangulates the irregular data using Delauny triangulation method, therewith interpolates each boundary and radial curve of the triangle by C^1 rational trigonometric cubic function. Half of the parameters in the description of the interpolant are constrained to keep up the positive shape of data while the remaining half are set free for users' requirement. Orthogonality of trigonometric function assures much smoother surface as compared to polynomial functions. The proposed scheme can be of great use in areas of surface reconstruction and deformation, signal processing, CAD/CAM design, solving differential equations, and image restoration.

Citation: Ibraheem F, Hussain MZ, Bhatti AA (2015) C^1 Positive Surface over Positive Scattered Data Sites. PLoS ONE 10(6): e0120658. doi:10.1371/journal.pone.0120658

Academic Editor: Cheng-Yi Xia, Tianjin University of Technology, CHINA

Received: July 12, 2014

Accepted: February 5, 2015

Published: June 9, 2015

Data Availability Statement: All relevant data are within the paper.

Funding: The authors have no support or funding to report.

Competing Interests: The authors have declared that no competing interests exist.

1. Introduction

Data measured or amassed from many engineering and scientific fields, is often positioned at sparse points. For example, meteorological measurements at different weather stations [1], density measurements on different positions within the human body, heart potential measurements at random points in the diagnosis of various ailments of heart [2], 3D photography, aeronautical engineering and industrial design, structural graph networks [3], graph entropy [4], [5], [6]. A visual model is often required to get a clear understanding of underlying phenomena as colossal amount of data is difficult to analyse or communicate a message in raw form. Further, a meticulous visual representation obligates the interpolating function to affirm intrinsic attributes of data like positivity, monotonicity and convexity. Although, tensor product provides a robust medium for fitting surface to rectilinear data sites, it can not be used to fit a surface over sparse data points. This paper addresses the problem of retaining positivity over scattered data points.

Several approaches have been proposed in literature to address the problem of positivity preserving interpolating surfaces. Amidor [7] surveyed method to interpolate scattered data necessitating from electronic imaging system. The author mainly examined radial basis function method, tetrahedral interpolation, cubic triangular interpolation, triangle based blending interpolation, inverse distance method and neutral neighbourhood. The difference between

scattered data interpolation and scattered data fitting was also demonstrated in the survey. Cubic and quintic Hermite interpolants were used for preserving monotonicity, positivity and convexity of discrete data by [8]. Piah, Goodman, Unsworth [9] first triangulated the data points by Delaunay triangulation and constructed the interpolating surface consisting of "cubic Bezier triangular patches". Positivity of data was achieved by imposing sufficient conditions on Bezier ordinates in each triangular patch. The proposed scheme was local and C^1 continous. Hussain and Hussain [10] arranged the scattered data over a triangular grid to preserve the positivity and monotonicity. The authors used a cubic interpolant with one parameter to interpolate the boundary of each triangular patch while linear interpolant was used in Nielson side vertex method to obtain radial curves. Final surface patch was obtained by convex combination of interpolants. Positivity and monotonicity was retained by deriving data dependent constraints on free parameters. C^1 Quadratic splines and Powell-Sabin splines were used as interpolating function to tackle the problem of range restricted univariate and bivariate scattered data by Hermann et. al. [11]. The authors obtained a system of inequalities for the gradients and positivity was accomplished by deriving sufficient conditions on this system. A C^1 local rational cubic Bernstein Bezier interpolatory scheme was proposed by Hussain and Hussain [12] to retain positivity of scattered data. In each triangular patch, inner and boundary Bezier ordinates were confined for positivity. If in any triangular grid, Bezier ordinates failed to attain positive shape of data, then these were varied by the weights described in formation of rational cubic Bernstein Bezier interpolant. Sarfraz et. al. [1] established a local C^1 approach to keep up the positivity of scattered data positioned over a triangular domain. They employed C^1 rational cubic function with four parameters in Nielson side vertex technique to formulate the interpolating surface. Two of the four parameters were constrained for positivity.

Although several approaches have been proposed to retain the positivity of data, little attention has been paid towards the use of trigonometric basis function. This paper develops a positivity preserving scheme for scatter data by taking C^1 rational trigonometric function [13] into account. Delaunay triangulation method has been used to place scatter data as vertices of triangle. Nielson side vertex method [14] has been employed in each triangle to construct triangular patches. The C^1 rational trigonometric cubic function [13] with four parameter has been used for the interpolation along boundary and radial curve of the triangle. Positivity is attained by deriving data dependent condition on half of the parameters in the description of C^1 rational trigonometric cubic function [13].

The remainder of the paper is formulated as: Section 2 reviews the ratonal trigonometric cubic function [13]. Nielson side vertex method [14] to formulate triangular patches is detailed in Section 3. Positivity preserving algorithm is developed and explained in Section 4. Section 5 demonstrates the developed algorithm and presents graphical results. Section 5 summarizes this research and draws conclusion.

2. Rational Trigonometric Cubic Function

Let $\{(x_i, y_i), i = 0,1,2, \ldots, n-1\}$ be the given set of data points defined over the interval $[a, b]$ where $a = x_0 < x_1 < x_2 < \ldots < x_n = b$. A piecewise rational trigonometric cubic function is defined over each subinterval $I_i = [x_i, x_{i+1}]$ as

$$S_i(x) = \frac{p_i(\theta)}{q_i(\theta)} \tag{1}$$

$$
\begin{aligned}
p_i(\theta) &= \alpha_i f_i(1-\sin\theta)^3 + \left\{\beta_i f_i + \frac{2h_i\alpha_i d_i}{\pi}\right\}\sin\theta(1-\sin\theta)^2 \\
&+ \left\{\gamma_i f_{i+1} - \frac{2h_i\delta_i d_{i+1}}{\pi}\right\}\cos\theta(1-\cos\theta)^2 + \delta_i f_{i+1}(1-\cos\theta)^3 \\
q_i(\theta) &= \alpha_i(1-\sin\theta)^3 + \beta_i\sin\theta(1-\sin\theta)^2 + \gamma_i\cos\theta(1-\cos\theta)^2 + \delta_i(1-\cos\theta)^3
\end{aligned}
$$

where

$$
\theta = \frac{\pi}{2}\left(\frac{x-x_i}{h_i}\right), h_i = x_{i+1} - x_i, \quad i = 0, 1, 2, ..., n-1
$$

The rational trigonometric cubic function (Eq 1) satisfy the following properties:

$$
S(x_i) = f_i, S(x_{i+1}) = f_{i+1}, S'(x_i) = d_i, S'(x_{i+1}) = d_{i+1}. \tag{2}
$$

d_i and d_{i+1} are derivative at the endpoints of the interval $I_i = [x_i, x_{i+1}]$. α_i, β_i, γ_i and δ_i are the free parameters. The following result has been proved in [13].

Theorem 2.1 *The C^1 piecewise rational trigonometric cubic function preserve the positivity of positive data if in each subinterval $I_i = [x_i, x_{i+1}]$, the parameters β_i and γ_i satisfy the following sufficient conditions*

$$
\beta_i = u_i + \max\left\{0, \frac{-2h_i d_i\alpha_i}{\pi f_i}\right\}, u_i > 0,
$$

$$
\gamma_i = v_i + \max\left\{0, \frac{2h_i d_{i+1}\delta_i}{\pi f_{i+1}}\right\}, v_i > 0.
$$

3. Nielson Side Vertex Method

Consider a triangle $\triangle V_1\, V_2\, V_3$ with vertices V_1, V_2, V_3 having edges e_1, e_2, e_3 and u, v, w be the barycentric coordinates such that any point V on the triangle can be written as:

$$
V \doteq uV_1 + vV_2 + wV_3, \tag{3}
$$

where

$$
u + v + w = 1 \text{ and } u, v, w \geq 0.
$$

The interpolant defined by Nielson [14] to generate surface over each triangular patch is defined as the following convex combination:

$$
P(a,b,c) = \frac{v^2w^2Q_1 + u^2w^2Q_2 + u^2v^2Q_3}{v^2w^2 + u^2w^2 + u^2v^2}. \tag{4}
$$

where $Q_i's$ represent line segments joining vertices $V_i's$ to points $S_i's$ on the opposite boundary. Eq (4) interpolates data at the vertices as well as first order derivatives at the boundary. Since the barycentric coordinates at the vertices of triangle is simultaneously zero, the interpolant Eq (4) takes the following values:

$$
P(a,b,c) = Q_1 \text{ when } v = w = 0,
$$

$$
P(a,b,c) = Q_2 \text{ when } u = w = 0,
$$

$$
P(a,b,c) = Q_3, \text{ when } v = u = 0,
$$

where Q_i, i = 1,2,3 are the ordinate values at the vertices V_i, i = 1,2,3 of triangle.

4. Positive Scatter Data Interpolation

This section details the derivation of sufficient conditions for C^1 triangular patches to be positive. Let the given positive scattered data set arranged over a triangular domain be $\{(x_i, y_i, F_i), i = 1,2, \ldots, n\}$. The resulting surface $S(x, y)$ described as

$$S(x_i, y_i) = F_i, i = 1, 2, ..., n, \tag{5}$$

is positive if

$$S(x, y) > 0, \forall (x, y) \in D. \tag{6}$$

4.1 Domain Triangulation

Triangulation of data is performed by Delaunay triangulation method such that data F_i, fall on vertices $\{V_i = (x_i, y_i), i = 1,2,3, \ldots, n\}$ of the triangles.

4.2 Estimation of Derivatives

Partial derivatives at the vertices V_i, $i = 1,2,3$ of each triangle are calculated by derivative estimation scheme suggested by Goodman et. al. [15]

4.3 C^1 Positive triangular patch

Let $V_1\ V_2\ V_3$ be the given triangle with edges e_i, $i = 1,2,3$ opposite to the vertices V_i, $i = 1,2,3$ respectively and S_i, $i = 1,2,3$ be the points on the edges opposite to vertices V_i, $i = 1,2,3$. The radial curve Q_1 connecting vertex V_1 to the points S_1 on the opposite edges e_1 is defined as (Fig 1):

$$Q_1 = \frac{Q_{1n}}{Q_{1d}}, \tag{7}$$

where

$$\begin{aligned} Q_{1n} &= (1 - \sin\lambda)^3 F_1\alpha_1 + \sin\lambda(1 - \sin\lambda)^2\left(\beta_1 F_1 + \frac{2R_1\alpha_1}{\pi}\right) \\ &+ \cos\hat{\lambda}(1 - \cos\hat{\lambda})^2\left(\gamma_1 F(S_1) - \frac{2\delta_1 R_2}{\pi}\right) + (1 - \cos\hat{\lambda})^3\delta_1 F(S_1), \\ Q_{1d} &= \alpha_1(1 - \sin\lambda)^3 + \beta_1 \sin\lambda(1 - \sin\lambda)^2 + \gamma_1 \cos\hat{\lambda}(1 - \cos\hat{\lambda})^2 + \delta_1(1 - \cos\hat{\lambda})^3. \end{aligned}$$

such that

$$\lambda = \frac{\pi}{2}(1 - u), \hat{\lambda} = 1 - \lambda.$$

R_1 and R_2 are the directional derivatives at V_1 and S_1 (Fig 2) defined as

$$\begin{aligned} R_1 &= (x_{s_1} - x_1)\frac{\partial f}{\partial x}(V_1) + (y_{s_1} - y_1)\frac{\partial f}{\partial y}(V_1), \\ R_2 &= (x_{s_1} - x_1)\frac{\partial f}{\partial x}(S_1) + (y_{s_1} - y_1)\frac{\partial f}{\partial y}(S_1). \end{aligned}$$

and $F(S_1)$ is the boundary curve along the edge e_1 evaluated from the following expression

$$F(S_1) = \frac{F_{1n}}{F_{1d}},$$

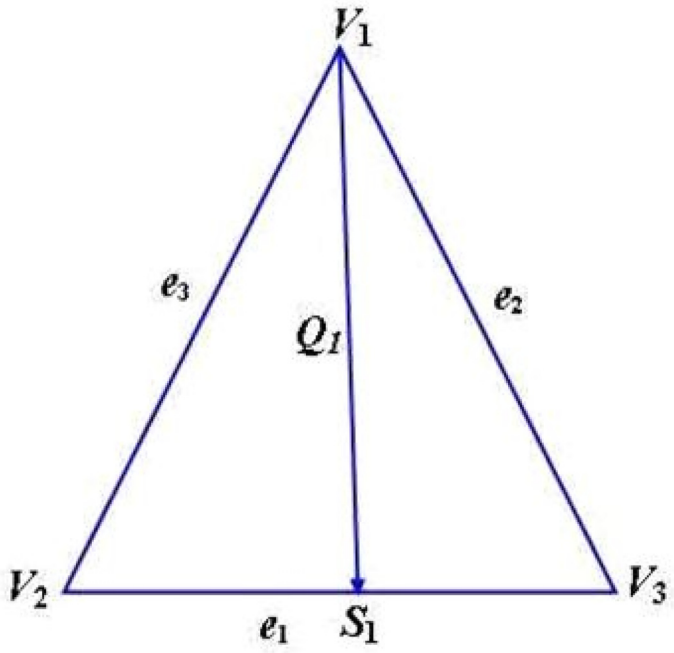

Fig 1. Radial curve Q_1: connecting vertex V_1 to the point S_1.

doi:10.1371/journal.pone.0120658.g001

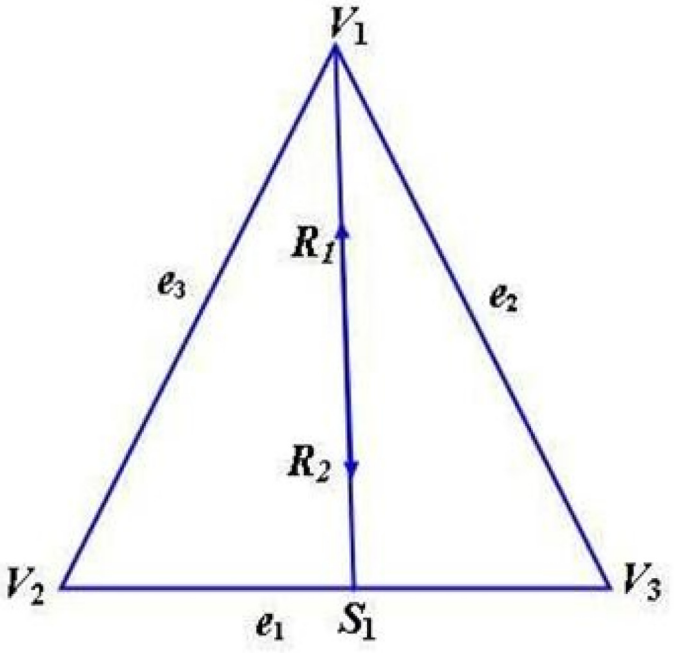

Fig 2. Directional derivatives along $\overrightarrow{S_1V_1}$.

doi:10.1371/journal.pone.0120658.g002

where

$$\begin{aligned} F_{1n} &= (1-\sin r)^3 F_2\alpha_4 + \sin r(1-\sin r)^2\left(\beta_4 F_2 + \frac{2d_3\alpha_4}{\pi}\right) \\ &+ \cos\hat{r}(1-\cos\hat{r})^2\left(\gamma_4 F_3 - \frac{2\delta_4 d_4}{\pi}\right) + (1-\cos\hat{r})^3\delta_4 F_3, \\ F_{1d} &= \alpha_4(1-\sin r)^3 + \beta_4 \sin r(1-\sin r)^2 + \gamma_4\cos\hat{r}(1-\cos\hat{r})^2 + \delta_4(1-\cos\hat{r})^3. \end{aligned}$$

such that

$$r = \frac{\pi(1-v)}{2(v+w)}, \hat{r} = \frac{\pi(1-w)}{2(u+w)}.$$

d_3 and d_4 are the directional derivatives along $\overrightarrow{V_2V_3}$ at V_2 and V_3 (Fig 3)

$$d_3 = (x_3 - x_2)\frac{\partial f}{\partial x}(V_2) + (y_3 - y_2)\frac{\partial f}{\partial y}(V_2),$$
$$d_4 = (x_3 - x_2)\frac{\partial f}{\partial x}(V_3) + (y_3 - y_2)\frac{\partial f}{\partial y}(V_3).$$

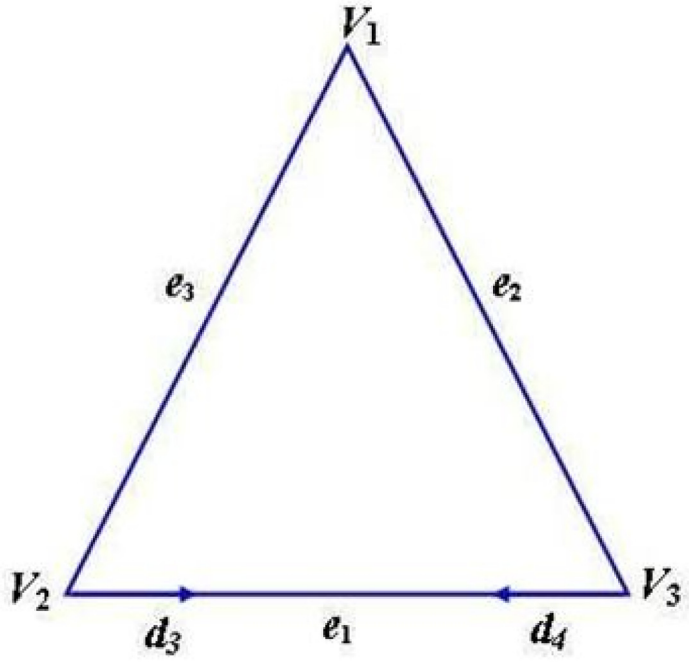

Fig 3. Directional derivatives along $\overrightarrow{V_2V_3}$

doi:10.1371/journal.pone.0120658.g003

From Eq 7, $Q_1 > 0$ if

$$Q_{1n} > 0 \text{ and } Q_{1d} > 0.$$

Now, $Q_{1n} > 0$ if

$$\begin{aligned} \alpha_1 > 0,\ \delta_1 > 0, \\ \beta_1 > \frac{-2R_1\alpha_1}{\pi F_1}, \\ \gamma_1 > \frac{2R_2\delta_1}{\pi F(S_1)}, \\ F(S_1) > 0 \quad . \end{aligned} \tag{8}$$

From Theorem 2.1, $F(S_1) > 0$ if

$$\beta_4 > \frac{-2\alpha_4 d_3}{\pi F_2}, \gamma_4 > \frac{2\delta_4 d_4}{\pi F_3}. \tag{9}$$

Now, $Q_{1d} > 0$ if

$$\alpha_1 > 0, \beta_1 > 0, \gamma_1 > 0 \text{ and } \delta_1 > 0.$$

Likewise, radial curve Q_2 connecting vertex V_2 to the points S_2 on the opposite edges e_2 is defined as

$$Q_2 = \frac{Q_{2n}}{Q_{2d}}, \tag{10}$$

where

$$\begin{aligned} Q_{2n} &= (1 - \sin\mu)^3 F_2\alpha_2 + \sin\mu(1 - \sin\mu)^2\left(\beta_2 F_2 + \frac{2R_3\alpha_2}{\pi}\right) \\ &+ \cos\hat{\mu}(1 - \cos\hat{\mu})^2\left(\gamma_2 F(S_2) - \frac{2\delta_2 R_4}{\pi}\right) + (1 - \cos\hat{\mu})^3\delta_2 F(S_2), \\ Q_{2d} &= \alpha_2(1 - \sin\mu)^3 + \beta_2 \sin\mu(1 - \sin\mu)^2 + \gamma_2 \cos\hat{\mu}(1 - \cos\hat{\mu})^2 + \delta_2(1 - \cos\hat{\mu})^3. \end{aligned}$$

such that

$$\mu = \frac{\pi}{2}(1 - \nu), \hat{\mu} = 1 - \mu. \tag{11}$$

R_3 and R_4 are the directional derivatives at V_2 and S_2

$$\begin{aligned} R_3 &= (x_{s_2} - x_2)\frac{\partial f}{\partial x}(V_2) + (y_{s_2} - y_2)\frac{\partial f}{\partial y}(V_2) \\ R_4 &= (x_{s_2} - x_2)\frac{\partial f}{\partial x}(S_2) + (y_{s_2} - y_2)\frac{\partial f}{\partial y}(S_2) \end{aligned}$$

and $F(S_2)$ is the boundary curve along the edge e_2 to be evaluated from the following expression

$$F(S_2) = \frac{F_{2n}}{F_{2d}},$$

where

$$\begin{aligned} F_{2n} &= (1-\sin s)^3 F_3\alpha_5 + \sin r(1-\sin r)^2\left(\beta_5 F_3 + \frac{2d_5\alpha_5}{\pi}\right) \\ &+ \cos r(1-\cos r)^2\left(\gamma_5 F_1 - \frac{2\delta_5 d_6}{\pi}\right) + (1-\cos r)^3\delta_5 F_1, \\ F_{2d} &= \alpha_5(1-\sin r)^3 + \beta_5 \sin r(1-\sin r)^2 + \gamma_5 \cos r(1-\cos r)^2 + \delta_5(1-\cos r)^3. \end{aligned}$$

d_5 and d_6 are the directional derivatives along $\overrightarrow{V_1V_3}$ at V_1 and V_3

$$\begin{aligned} d_5 &= (x_1-x_3)\frac{\partial f}{\partial x}(V_3) + (y_1-y_3)\frac{\partial f}{\partial y}(V_3), \\ d_6 &= (x_3-x_2)\frac{\partial f}{\partial x}(V_1) + (y_3-y_2)\frac{\partial f}{\partial y}(V_1). \end{aligned}$$

From Eq 10, $Q_2 > 0$ if

$$Q_{2n} > 0 \text{ and } Q_{2d} > 0.$$

Now, $Q_{2n} > 0$ if

$$\begin{aligned} &\alpha_2 > 0,\ \delta_2 > 0, \\ &\beta_2 > \frac{-2R_3\alpha_2}{\pi F_2}, \\ &\gamma_2 > \frac{2R_4\delta_2}{\pi F(S_2)}, \\ &F(S_2) > 0 \quad . \end{aligned} \tag{12}$$

From Theorem 2.1, $F(S_2) > 0$ if

$$\beta_5 > \frac{-2\alpha_5 d_5}{\pi F_3}, \gamma_5 > \frac{2\delta_5 d_6}{\pi F_1}. \tag{13}$$

Now, $Q_{2d} > 0$ if

$$\alpha_2 > 0, \beta_2 > 0, \gamma_2 > 0 \text{and} \delta_2 > 0.$$

and the radial curve Q_3 connecting vertex V_3 to the point S_3 on the opposite edge e_3 is defined as

$$Q_3 = \frac{Q_{3n}}{Q_{3d}}, \tag{14}$$

where

$$\begin{aligned} Q_{3n} &= (1-\sin v)^3 F_3\alpha_3 + \sin v(1-\sin v)^2\left(\beta_3 F_3 + \frac{2R_5\alpha_3}{\pi}\right) \\ &+ \cos v(1-\cos v)^2\left(\gamma_3 F(S_3) - \frac{2\delta_3 R_6}{\pi}\right) + (1-\cos v)^3\delta_3 F(S_3), \\ Q_{3d} &= \alpha_3(1-\sin v)^3 + \beta_3 \sin v(1-\sin v)^2 + \gamma_3 \cos v(1-\cos v)^2 + \delta_3(1-\cos v)^3. \end{aligned}$$

where R_5 and R_6 are the directional derivatives at V_3 and S_3 defined as

$$\begin{aligned} R_5 &= (x_{s_3} - x_3)\frac{\partial f}{\partial x}(V_3) + (y_{s_3} - y_3)\frac{\partial f}{\partial y}(V_3) \\ R_6 &= (x_{s_3} - x_3)\frac{\partial f}{\partial x}(S_3) + (y_{s_3} - y_3)\frac{\partial f}{\partial y}(S_3) \end{aligned}$$

and $F(S_3)$ is the boundary curve along the edge e_3 to be evaluated from the following expression

$$F(S_3) = \frac{F_{3n}}{F_{3d}},$$

where

$$\begin{aligned} F_{3n} &= (1 - \sin t)^3 F_1 \alpha_6 + \sin t(1 - \sin t)^2 \left(\beta_6 F_1 + \frac{2d_1\alpha_6}{\pi}\right) \\ &+ \cos t(1 - \cos t)^2 \left(\gamma_6 F_2 - \frac{2\delta_6 d_2}{\pi}\right) + (1 - \cos t)^3 \delta_6 F_2, \\ F_{3d} &= \alpha_6(1 - \sin t)^3 + \beta_6 \sin t(1 - \sin t)^2 + \gamma_6 \cos t(1 - \cos t)^2 + \delta_6(1 - \cos t)^3. \end{aligned}$$

d_1 and d_2 are the directional derivatives along $\overrightarrow{V_1V_2}$ at V_1 and V_2

$$\begin{aligned} d_5 &= (x_2 - x_1)\frac{\partial f}{\partial x}(V_1) + (y_2 - y_1)\frac{\partial f}{\partial y}(V_1), \\ d_6 &= (x_2 - x_1)\frac{\partial f}{\partial x}(V_2) + (y_2 - y_1)\frac{\partial f}{\partial y}(V_2). \end{aligned}$$

From Eq 14, $Q_3 > 0$ if

$$Q_{3n} > 0 \text{ and } Q_{3d} > 0.$$

Now, $Q_{3n} > 0$ if

$$\begin{aligned} &\alpha_3 > 0,\ \delta_2 > 0, \\ &\beta_3 > \frac{-2R_5\alpha_3}{\pi F_3}, \\ &\gamma_3 > \frac{2R_6\delta_3}{\pi F(S_3)}, \\ &F(S_3) > 0 \quad . \end{aligned} \tag{15}$$

From Theorem 2.1, $F(S_3) > 0$ if

$$\beta_6 > \frac{-2\alpha_6 d_1}{\pi F_1}, \gamma_6 > \frac{2\delta_6 d_2}{\pi F_2}. \tag{16}$$

Now, $Q_{3d} > 0$ if

$$\alpha_3 > 0, \beta_3 > 0, \gamma_3 > 0 \text{ and } \delta_3 > 0.$$

The above discussion leads to the following result:

Theorem 4.1 *The C^1 triangular pactch P in Eq (4) is positive if the following conditions are attained.*

$$\alpha_1 > 0, \alpha_2 > 0, \alpha_3 > 0, \alpha_4 > 0, \alpha_5 > 0, \alpha_6 > 0,$$
$$\delta_1 > 0, \delta_2 > 0, \delta_3 > 0, \delta_4 > 0, \delta_5 > 0, \delta_6 > 0,$$
$$\beta_1 > \max\left\{0, \frac{-2R_1\alpha_1}{\pi F_1}\right\}, \gamma_1 > \max\left\{0, \frac{2R_2\delta_1}{\pi F(S_1)}\right\},$$
$$\beta_2 > \max\left\{0, \frac{-2R_3\alpha_2}{\pi F_2}\right\}, \gamma_2 > \max\left\{0, \frac{2R_4\delta_2}{\pi F(S_2)}\right\},$$
$$\beta_3 > \max\left\{0, \frac{-2R_5\alpha_3}{\pi F_3}\right\}, \gamma_3 > \max\left\{0, \frac{2R_6\delta_3}{\pi F(S_3)}\right\},$$
$$\beta_4 > \max\left\{0, \frac{-2\alpha_4 d_3}{\pi F_2}\right\}, \gamma_4 > \max\left\{0, \frac{2\delta_4 d_4}{\pi F_3}\right\},$$
$$\beta_5 > \max\left\{0, \frac{-2\alpha_5 d_5}{\pi F_3}\right\}, \gamma_5 > \max\left\{0, \frac{2\delta_5 d_6}{\pi F_1}\right\},$$
$$\beta_6 > \max\left\{0, \frac{-2\alpha_6 d_1}{\pi F_1}\right\}, \gamma_6 > \max\left\{0, \frac{2\delta_6 d_2}{\pi F_2}\right\}.$$

The above constraints can be rearranged as

$$\beta_1 > l_1 + \max\left\{0, \frac{-2R_1\alpha_1}{\pi F_1}\right\}, \gamma_1 > m_1 + \max\left\{0, \frac{2R_2\delta_1}{\pi F(S_1)}\right\}; l_1, m_1 > 0,$$
$$\beta_2 > l_2 + \max\left\{0, \frac{-2R_3\alpha_2}{\pi F_2}\right\}, \gamma_2 > m_2 + \max\left\{0, \frac{2R_4\delta_2}{\pi F(S_2)}\right\}; l_2, m_2 > 0,$$
$$\beta_3 > l_3 + \max\left\{0, \frac{-2R_5\alpha_3}{\pi F_3}\right\}, \gamma_3 > m_3 + \max\left\{0, \frac{2R_6\delta_3}{\pi F(S_3)}\right\}; l_3, m_3 > 0,$$
$$\beta_4 > l_4 + \max\left\{0, \frac{-2\alpha_4 d_3}{\pi F_2}\right\}, \gamma_4 > m_4 + \max\left\{0, \frac{2\delta_4 d_4}{\pi F_3}\right\}; l_4, m_4 > 0,$$
$$\beta_5 > l_5 + \max\left\{0, \frac{-2\alpha_5 d_5}{\pi F_3}\right\}, \gamma_5 > m_5 + \max\left\{0, \frac{2\delta_5 d_6}{\pi F_1}\right\}; l_5, m_5 > 0,$$
$$\beta_6 > l_6 + \max\left\{0, \frac{-2\alpha_6 d_1}{\pi F_1}\right\}, \gamma_6 > m_6 + \max\left\{0, \frac{2\delta_6 d_2}{\pi F_2}\right\}; l_6, m_6 > 0.$$

5. Numerical Examples

This section illustrates the positivity preserving scheme for scattered data devised in Section 4.3.

Example 5.1 *Positive scattered data is taken in Table 1. Fig 4 represents corresponding delaunay triangulations. The data is interpolated first by Eq (4) for arbitrary values of free parameters,* $\alpha_1 = 4.1$, $\alpha_2 = 3$;$\alpha_3 = 2.5$, $\alpha_4 = 1.6$, $\alpha_5 = 2.7$, $\alpha_6 = 2.8$, $\beta_1 = 3.8$, $\beta_2 = 2.4$, $\beta_3 = 4.2$, $\beta_4 = 2.5$, $\beta_5 = 1.5$, $\beta_6 = 4$, $\gamma_1 = 1$, $\gamma_2 = 6$, $\gamma_3 = 1$, $\gamma_4 = 2$, $\gamma_5 = 2$, $\gamma_6 = 3$, $\delta_1 = 1$, $\delta_2 = 3$, $\delta_3 = 3$, $\delta_4 = 1$, $\delta_5 = 2$, $\delta_6 = 1$. *The resulting surface is displayed in Fig 5. It is clear from Fig 5 that the inherent shape feature*

Table 1. A Positive scattered data set I.

x	y	F
0	0	0.7487
0	0.125	0.5779
0	0.25	0.4668
0	0.375	0.4042
0	0.625	0.4042
0	0.75	0.4668
0	0.875	0.5779
0	1	0.7487
0.125	0	0.5779
0.125	0.125	0.4248
0.125	0.5	0.251
0.125	0.625	0.2691
0.125	0.75	0.3252
0.125	1	0.5779
0.25	0	0.4668
0.25	0.125	0.3252
0.25	0.25	0.2331
0.25	0.375	0.1813
0.25	0.5	0.1645
0.25	0.875	0.3252
0.375	0.125	0.2691
0.375	0.25	0.1813
0.375	0.625	0.1317
0.375	0.75	0.1813
0.375	0.875	0.2691
0.375	1	0.4042
0.5	0	0.384
0.5	0.375	0.1157
0.5	0.625	0.1157
0.5	0.75	0.1645
0.5	0.875	0.251
0.5	1	0.384
0.625	0	0.4042
0.625	0.125	0.2691
0.625	0.375	0.1317
0.625	0.5	0.1157
0.625	0.625	0.1317
0.75	0	0.4668
0.75	0.125	0.3252
0.75	0.375	0.1813
0.75	0.75	0.2331
0.75	0.875	0.3252
x	y	z
0.875	0	0.5779
0.875	0.125	0.4248
0.875	0.375	0.2691
0.875	0.625	0.2691

(*Continued*)

Table 1. (*Continued*)

x	y	F
0.875	0.75	0.3252
0.875	0.875	0.4248
0.875	1	0.5779
1	0	0.7487
1	0.125	0.5779
1	0.25	0.4668
1	0.375	0.4042
1	0.5	0.384
1	0.625	0.4042
1	0.75	0.4668
1	0.875	0.5779
1	1	0.7487
0.75	1	0.4668

doi:10.1371/journal.pone.0120658.t001

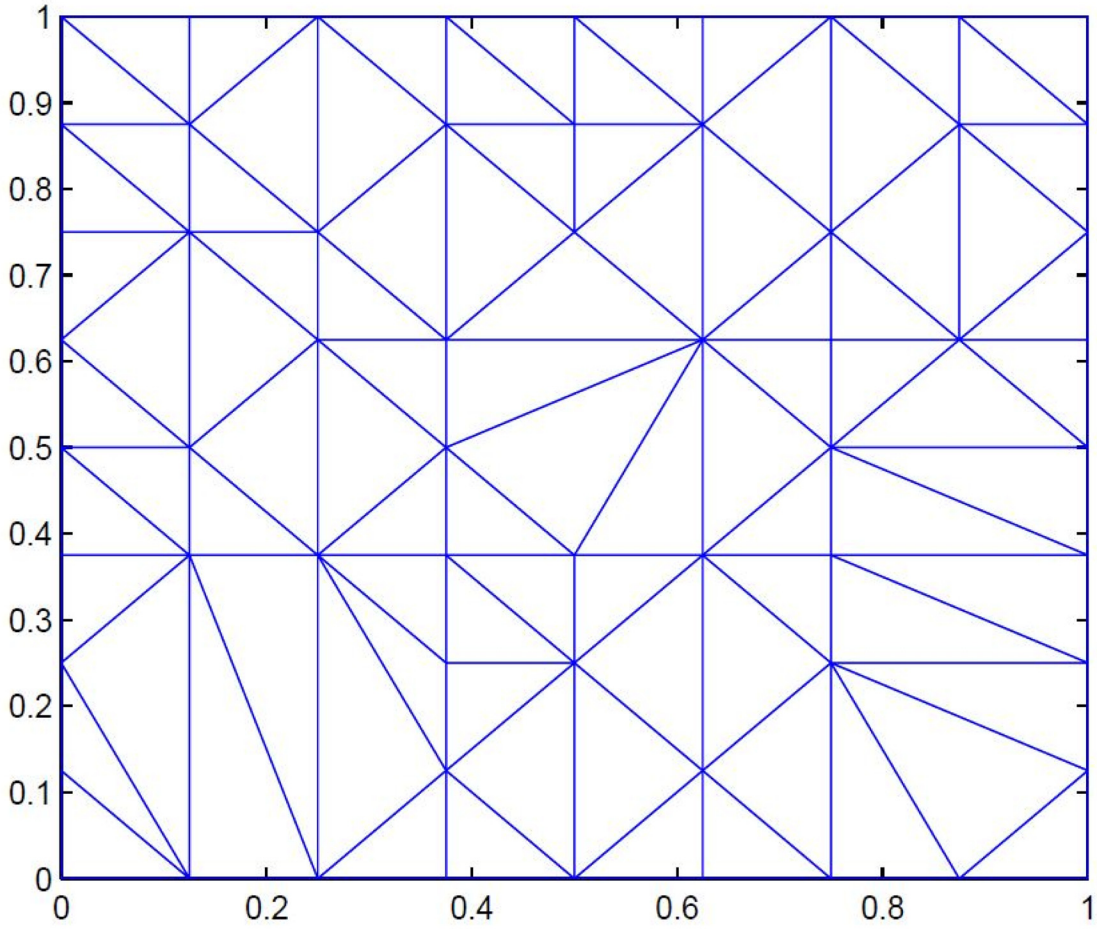

Fig 4. Delaunay triangulation of positive data in Table 1.

doi:10.1371/journal.pone.0120658.g004

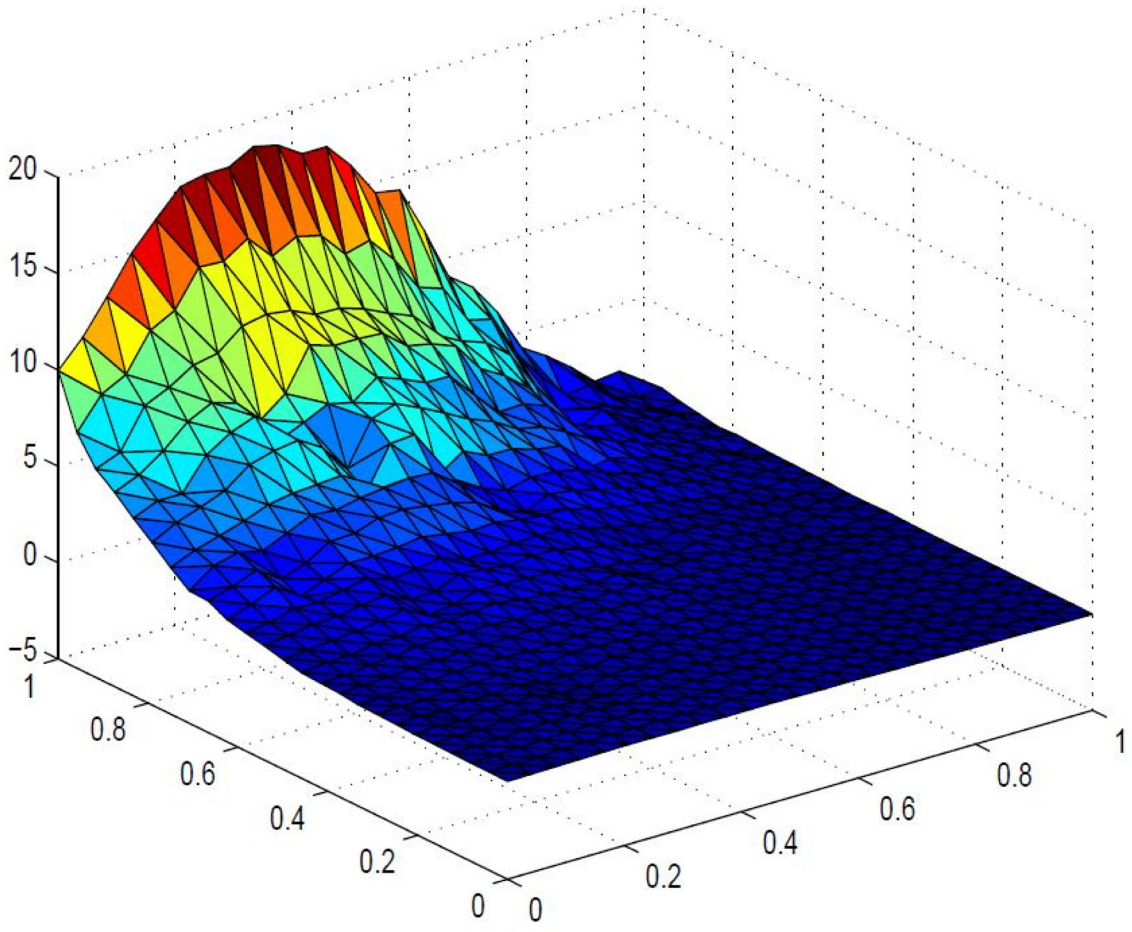

Fig 5. Rational cubic trigonometric surface of the positive data in Table 1.

doi:10.1371/journal.pone.0120658.g005

of positivity of data could no be held in visual model. This detriment is removed in Figs 6, 7 and 8 *by implementing positivity preserving conditions summarized in Theorem 4.1. It is worth mentioning here that parameters* α_i *and* δ_i *for* $i = 1,2,\ldots,6$ *are left free to refine the shape according to user's requirement. The effect of free parameters are shown in* Figs 6, 7 and 8. Figs 6 and 7 *are constructed against the parameter choice* $\alpha_1 = 12$, $\alpha_2 = 0.4$, $\alpha_3 = 13$, $\alpha_4 = 0.22$, $\alpha_5 = 12$, $\alpha_6 = 0.33$, $\delta_1 = 13$, $\delta_2 = 0.3$, $\delta_3 = 14$, $\delta_4 = 0.3$, $\delta_5 = 15$, $\delta_6 = 12$ and $\alpha_1 = 0.1$, $\alpha_2 = 1.0$, $\alpha_3 = 0.5$, $\alpha_4 = 1.6$, $\alpha_5 = 0.7$, $\alpha_6 = 0.8$, $\delta_1 = 0.8$, $\delta_2 = 0.4$, $\delta_3 = 1.2$, $\delta_4 = 1.5$, $\delta_5 = 1.5$, $\delta_6 = 1.0$ *respectively, which lacks smoothness. A smooth visibly pleasant representation is obtained in* Fig 8 *by setting* $\alpha_1 = 1.0$, $\alpha_2 = 1.0$, $\alpha_3 = 0.5$, $\alpha_4 = 0.6$, $\alpha_5 = 0.7$, $\alpha_6 = 0.8$, $\delta_1 = 0.8$, $\delta_2 = 0.4$, $\delta_3 = 1.2$, $\delta_4 = 0.5$, $\delta_5 = 1.0$, $\delta_6 = 1.0$

Example 5.2 *A Positive scattered data set is displayed in* Table 2. *Delauny triangulation is illustrated in* Fig 9 *and the corresponding surface in* Fig 10 *is obtained by interpolating the data*

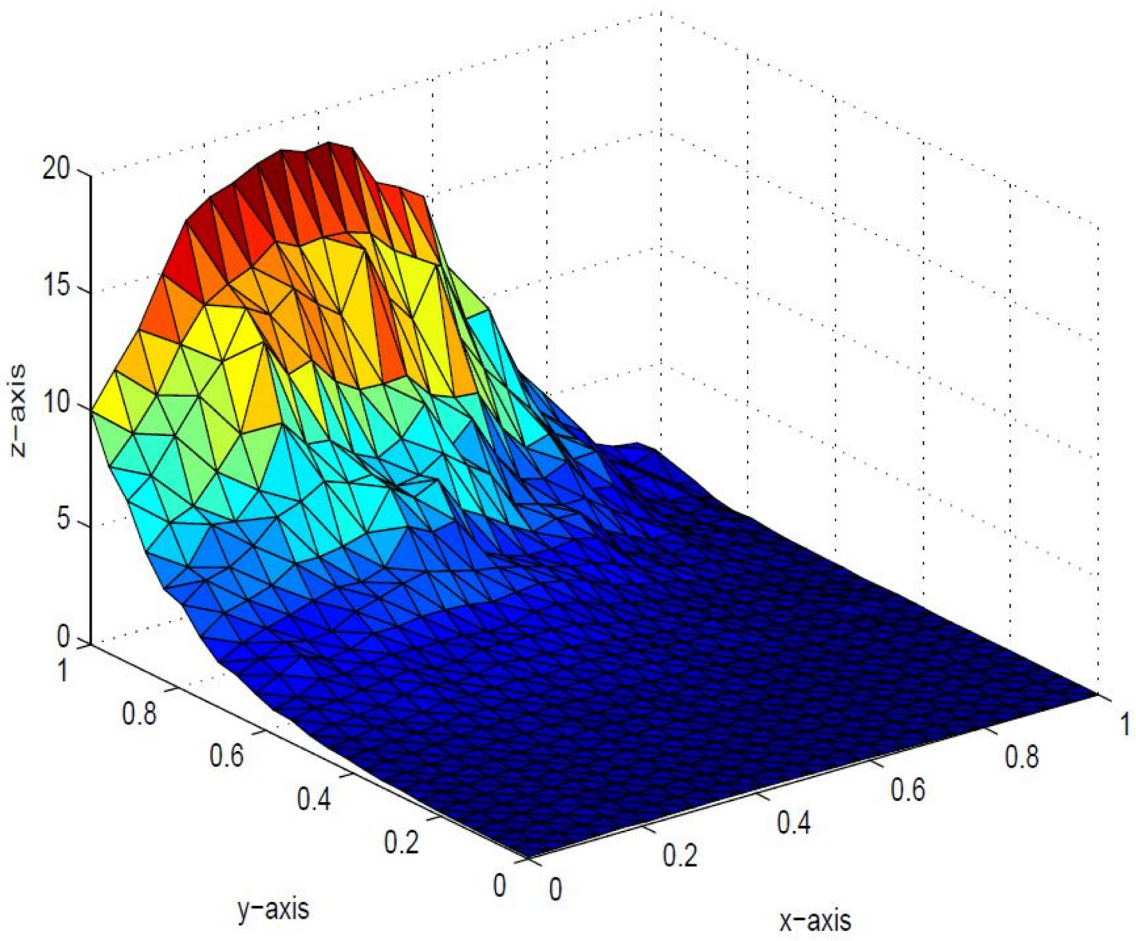

Fig 6. Positive surface generated from Theorem 4.1 of the positive data in Table 1.

doi:10.1371/journal.pone.0120658.g006

for arbitrary values of free parameters, $\alpha_1 = 4.1$, $\alpha_2 = 3$;$\alpha_3 = 2.0$, $\alpha_4 = 1.5$, $\alpha_5 = 2.7$, $\alpha_6 = 2.5$, $\beta_1 = 3.5$, $\beta_2 = 2.3$, $\beta_3 = 3.2$, $\beta_4 = 2.2$, $\beta_5 = 1.0$, $\beta_6 = 4.5$, $\gamma_1 = 1.4$, $\gamma_2 = 5.5$, $\gamma_3 = 1.5$, $\gamma_4 = 2.2$, $\gamma_5 = 1.5$, $\gamma_1 = 2.5$, $\delta_1 = 0.5$, $\delta_2 = 3.1$, $\delta_3 = 3.5$, $\delta_4 = 0.4$, $\delta_5 = 2$, $\delta_6 = 1.2$, *in description of Eq (4). It is evident from Fig 10 that the positivity of data could not be conserved in visual model. This impediment is removed in* Figs 11, 12 *and Fig 13 by implementing positivity preserving constraints on parameters* β_i, γ_i *for* $i = 1,2,\ldots,6$, *summarized in Theorem 4.1. Here, it is noteworthy that parameters* α_i *and* δ_i *for* $i = 1,2,\ldots,6$ *are set free to refine the shape as required by the user. The effect of free parameters are shown in* Figs 11, 12 and 13. Figs 11 *and* 12 *are constructed against the parameter choice* $\alpha_1 = 2.0$, $\alpha_2 = 0.1$, $\alpha_3 = 0.5$, $\alpha_4 = 0.5$, $\alpha_5 = 1.0$, $\alpha_6 = 0.63$, $\delta_1 = 1.0$, $\delta_2 = 0.33$, $\delta_3 = 0.5$, $\delta_4 = 0.4$, $\delta_5 = 1.0$, $\delta_6 = 0.3$ *and* $\alpha_1 = 2.2$, $\alpha_2 = 1.1$, $\alpha_3 = 2.5$, $\alpha_4 = 1.5$, $\alpha_5 = 1.0$, $\alpha_6 = 1.0$, $\delta_1 = 1.0$, $\delta_2 = 1.0$, $\delta_3 = 1.5$, $\delta_4 = 1.4$, $\delta_5 = 1.0$, $\delta_6 = 0.3$ *respectively, which lacks smoothness. A smooth visibly pleasant representation is obtained in Fig 13 by setting* $\alpha_1 = 2.0$, $\alpha_2 = 0.4$, $\alpha_3 = 0.5$, $\alpha_4 = 0.5$, $\alpha_5 = 1.0$, $\alpha_6 = 0.63$, $\delta_1 = 0.3$, $\delta_2 = 0.33$, $\delta_3 = 0.5$, $\delta_4 = 0.3$, $\delta_5 = 0.5$, $\delta_6 = 0.2$.

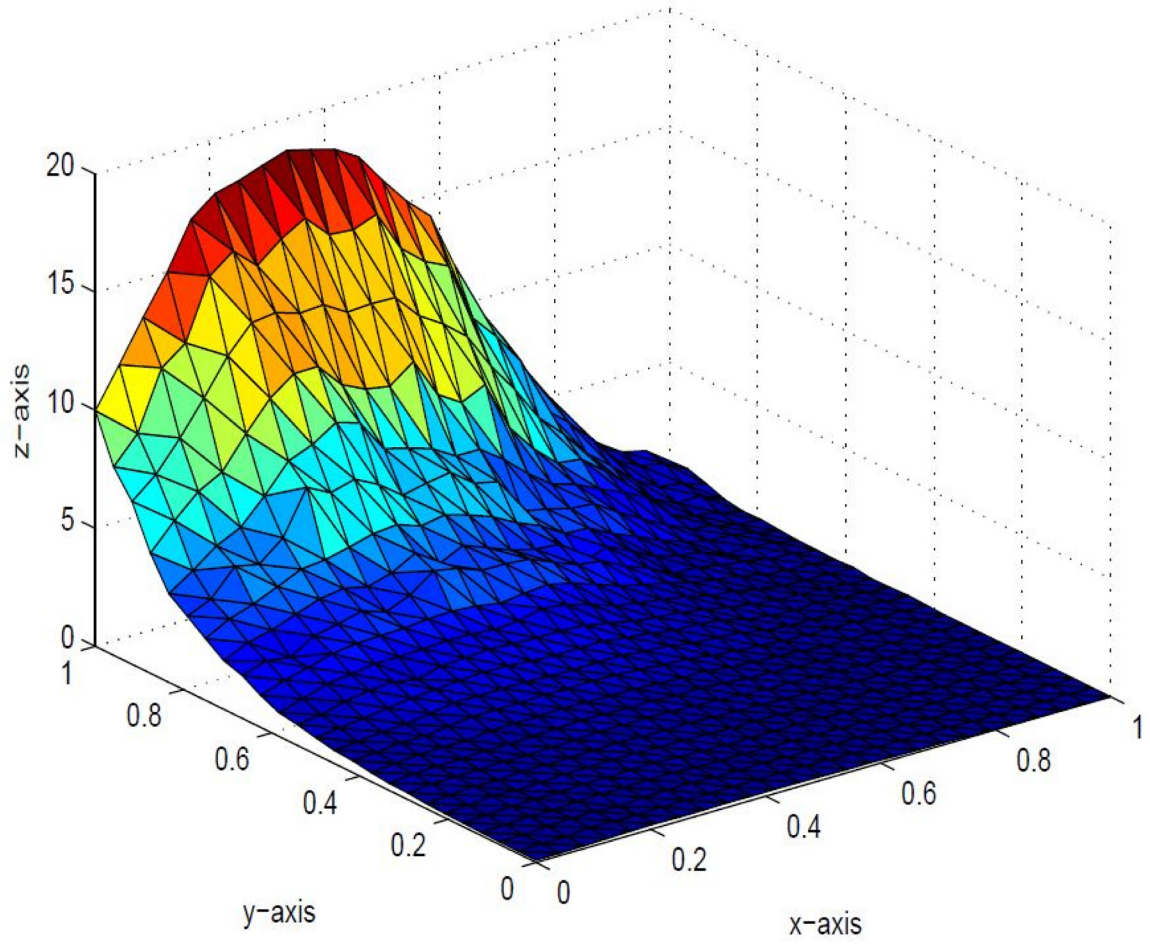

Fig 7. Positive surface generated from Theorem 4.1 of the positive data in Table 1.

doi:10.1371/journal.pone.0120658.g007

Conclusion

In this study, positivity preserving algorithm for scattered data arranged over a triangular domain, is established. The rational trigonometric cubic function [13] with four free parameters is used for the interpolation along each boundary and radial curve. Nielson side vertex has been applied to construct the interpolating surface. Constraints on half of the parameters are obtained to guarantee the positive shape of data while half are set free for users modification. The proposed algorithm, surpasses many prevailing approaches in literature. In [10], authors

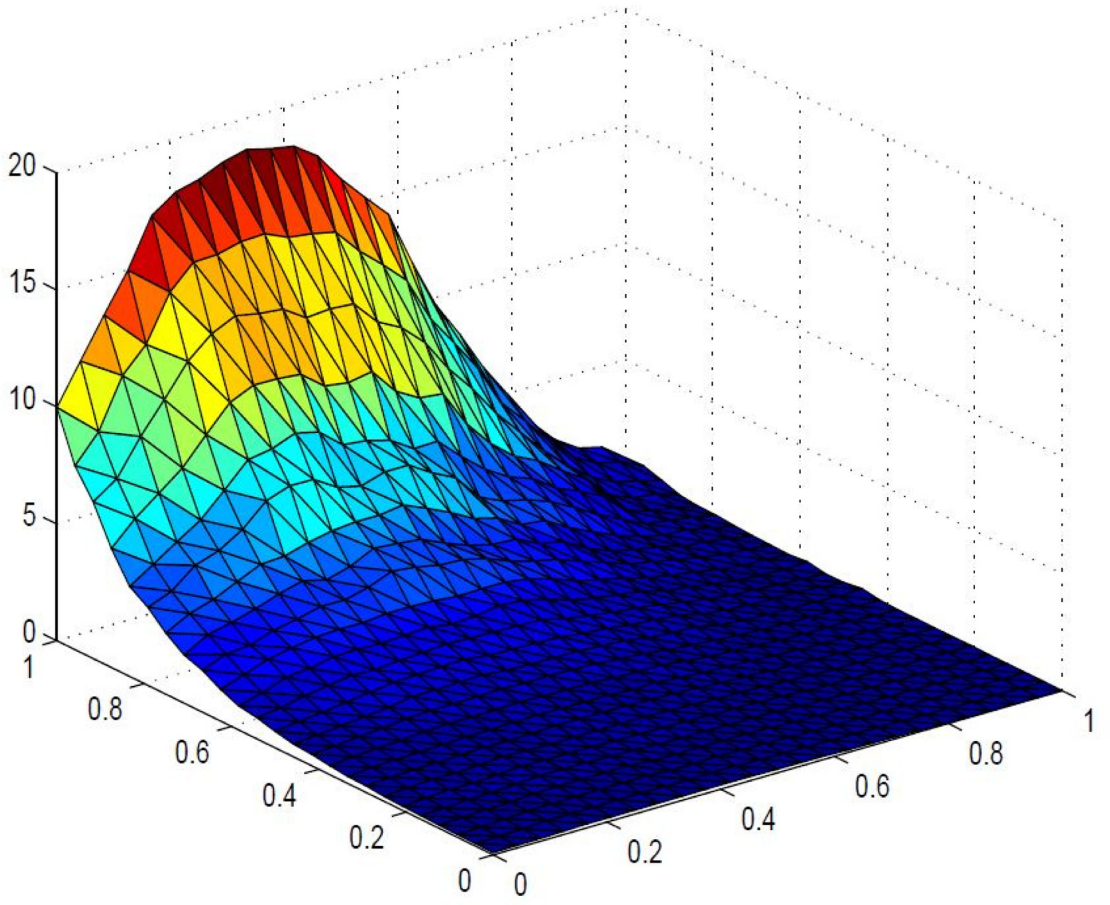

Fig 8. Positive surface generated from Theorem 4.1 of the positive data in Table 1.

doi:10.1371/journal.pone.0120658.g008

Table 2. A Positive scattered data set II.

x	y	F
0	0	0.4486
0	0.125	0.3616
0	0.25	0.4692
0	0.375	0.6827
0	0.5	0.786
0	0.625	0.836
0	0.75	0.8765
0	0.875	0.9125
0	1	0.9447
0.125	0	0.3369
0.125	0.125	0.0001
0.125	0.375	0.6256
0.125	0.625	0.8621

(*Continued*)

Table 2. (*Continued*)

x	y	F
0.125	0.875	0.9334
0.125	1	0.9634
0.25	0	0.4529
0.25	0.125	0.1767
0.25	0.25	0.3217
0.25	0.375	0.7005
0.25	0.5	0.8555
0.25	0.625	0.9327
0.25	0.75	0.9775
0.25	0.875	0.9686
0.25	1	0.9926
0.375	0	0.696
0.375	0.375	0.8363
0.375	0.625	1.2176
0.375	0.875	1.028
0.375	1	1.0284
0.5	0	0.8329
0.5	0.125	0.8315
0.5	0.25	0.821
0.5	0.375	0.8498
0.5	0.5	0.925
0.5	0.625	1.0925
0.5	0.75	1.1688
0.5	0.875	1.0568
0.5	1	1.0662
0.625	0	0.9049
0.625	0.125	0.8376
0.625	0.375	0.7163
0.625	0.5	0.8608
0.625	0.75	1.0671
0.625	0.875	1.0883
0.625	1	1.1023
0.75	0	0.9639
0.75	0.125	0.8326
0.75	0.25	0.6283
0.75	0.375	0.5976
0.75	0.5	0.8075
0.75	0.625	1.0136
0.75	0.75	1.0989
0.75	0.875	1.1231
0.75	1	1.134
0.875	0	1.0355
0.875	0.125	0.922
0.875	0.25	0.7477
0.875	0.375	0.7193
0.875	0.5	0.893
0.875	0.625	1.0638

(*Continued*)

Table 2. (*Continued*)

x	y	F
0.875	0.75	1.1335
0.875	0.875	1.152
0.875	1	1.1597
1	0	1.1074
1	0.125	1.0598
1	0.25	0.9848
1	0.375	0.9745
1	0.5	1.054
1	0.625	1.1319
1	0.75	1.1646
1	0.875	1.1744
1	1	1.1791

doi:10.1371/journal.pone.0120658.t002

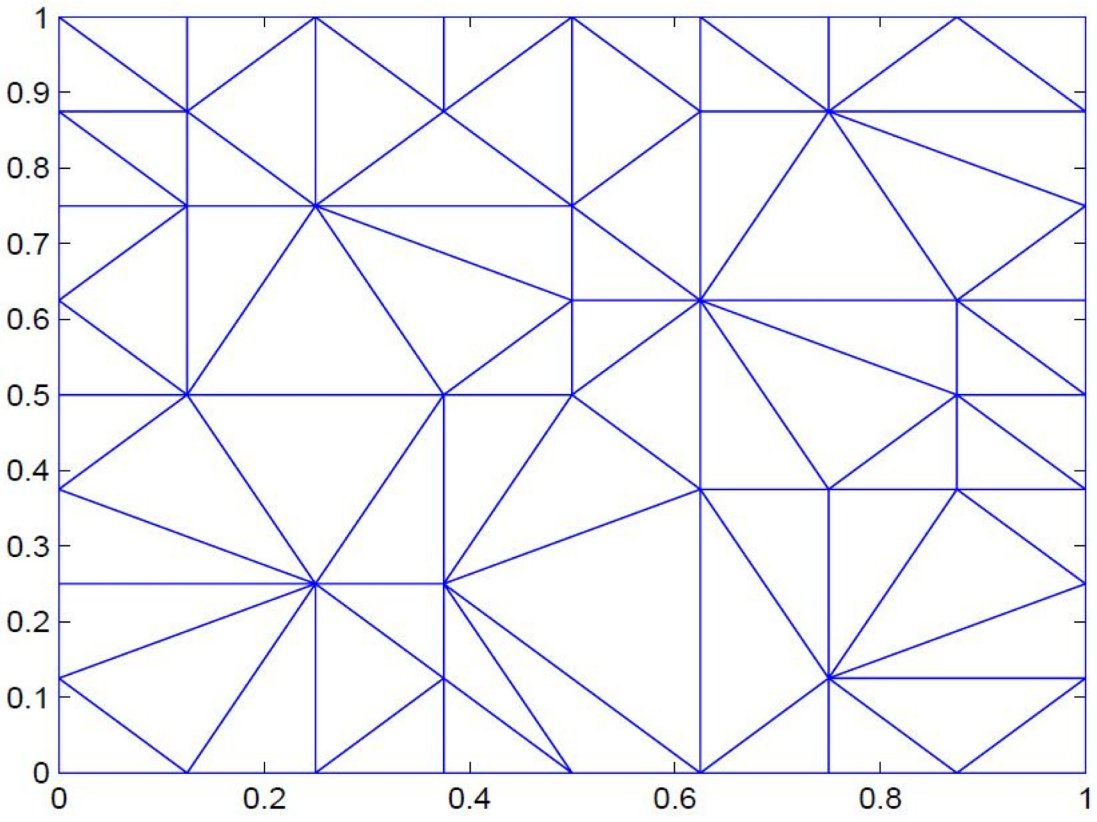

Fig 9. Delaunay triangulation of positive data in Table 2.

doi:10.1371/journal.pone.0120658.g009

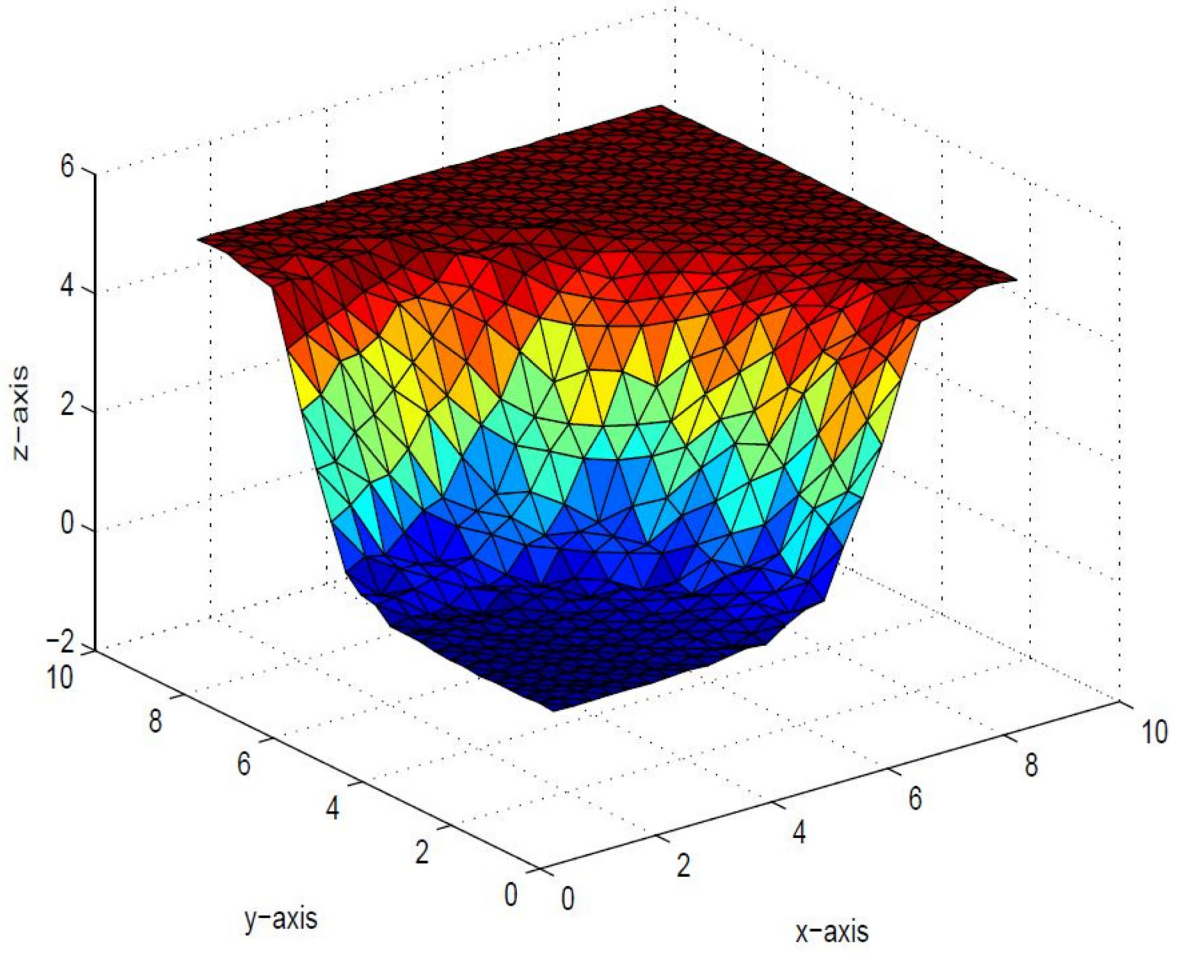

Fig 10. Rational cubic trigonometric surface of the positive data.

doi:10.1371/journal.pone.0120658.g010

utilized a cubic function with one free parameter to retain the positive shape of data. Positive surface was obtained by drawing data dependent constraints on this free parameter, and, hence the scheme did not offer refinement in the shape. The scheme suggested in this paper does not suffer this detriment. The developed algorithm is local and can be applied to data with or without derivatives. Moreover, shape preserving algorithms play an instrumental role in many areas of visualization such as geometric modelling, robot trajectories, evolution game theory, prisoner's dilemma game [16], [17], [18], meshless method and inverse kinemaics etc.

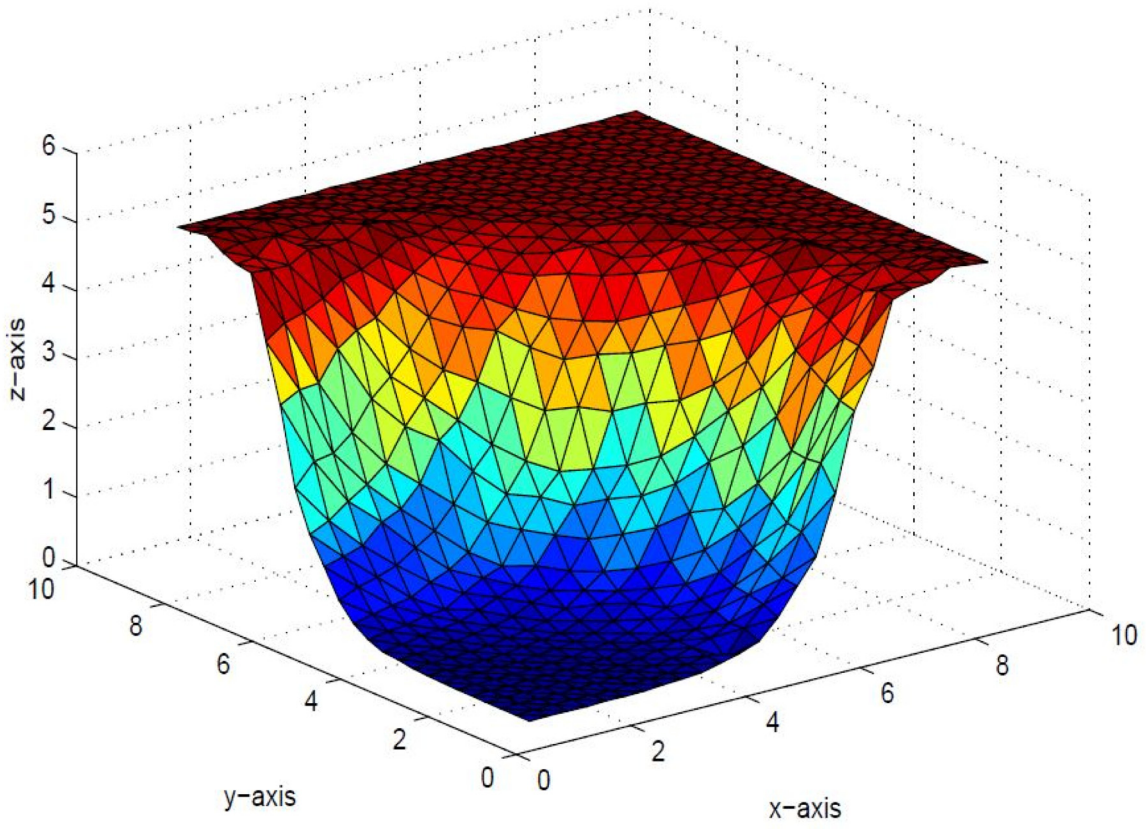

Fig 11. Positive surface generated from Theorem 4.1.

doi:10.1371/journal.pone.0120658.g011

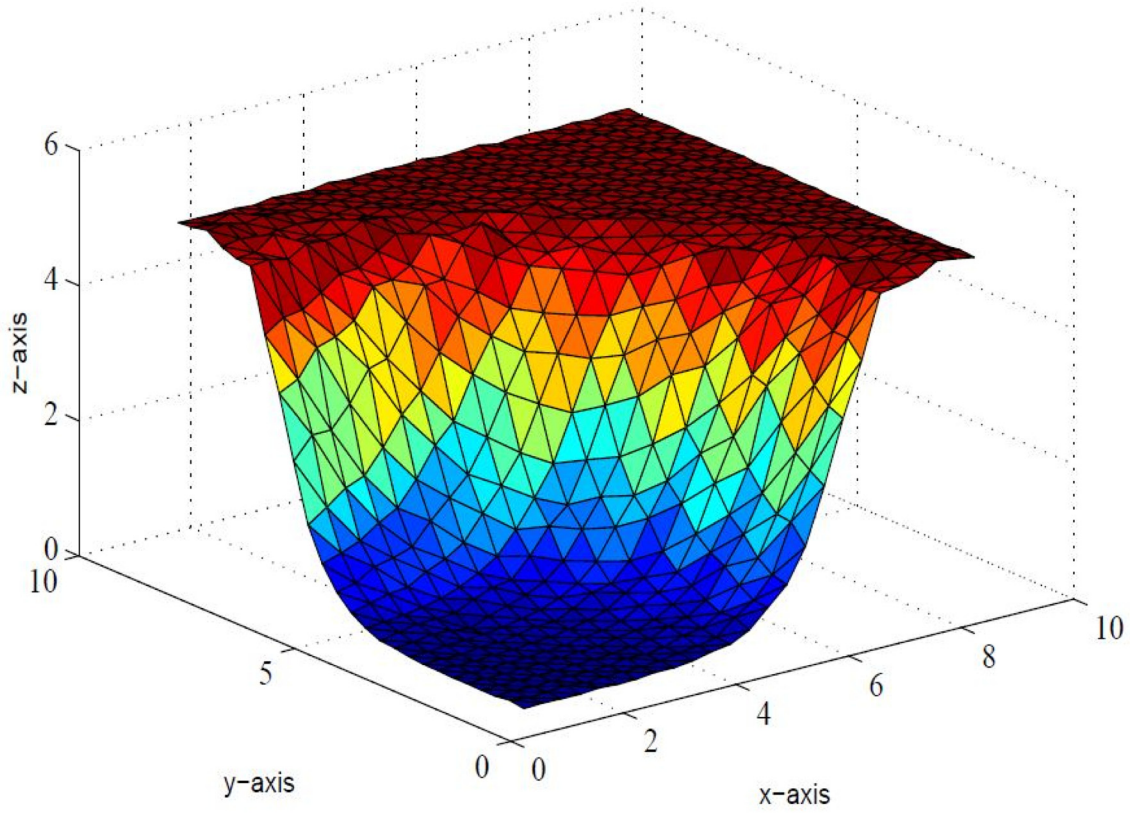

Fig 12. Positive surface generated from Theorem 4.1.

doi:10.1371/journal.pone.0120658.g012

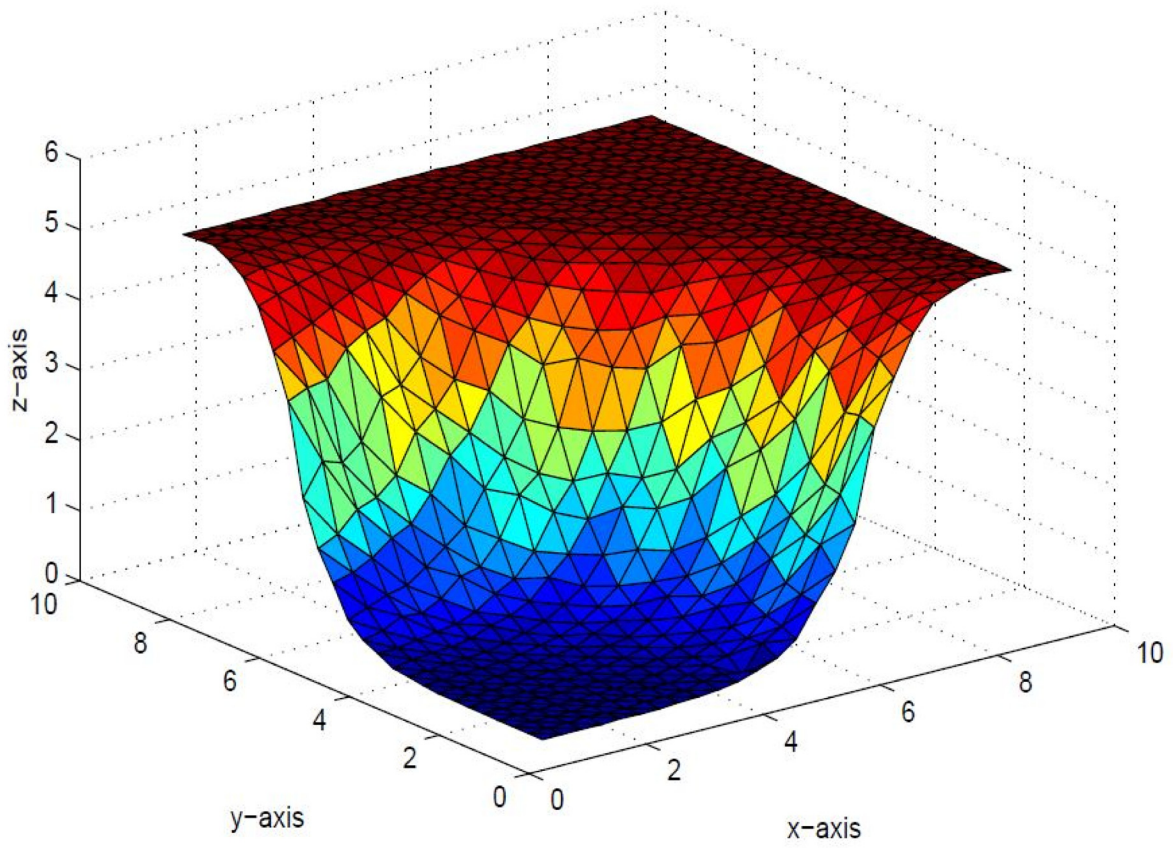

Fig 13. Positive surface generated from Theorem 4.1.

doi:10.1371/journal.pone.0120658.g013

Author Contributions

Conceived and designed the experiments: FI MZH AB. Performed the experiments: FI MZH AB. Analyzed the data: FI MZH AB. Contributed reagents/materials/analysis tools: FI MZH AB. Wrote the paper: FI MZH AB.

References

1. Sarfraz M, Hussain MZ, Arfan M. Positivty preserving scattered data interpolation scheme using the side vertex method. Applied Mathematics and Computation. 2012; 218(15):7898–7910. doi: 10.1016/j.amc.2012.01.072
2. Franke R, Nielson GM. Smooth interpolation of larger sets of scattered data. International Journal of Numerical Methods in Engineering. 1980; 15:1691–1704. doi: 10.1002/nme.1620151110
3. Kraus V, Dehmer M, Emmert-Streib F. Probabilistic inequalities for evaluating structural network measures. Information Sciences. 2014; 288:220–245. doi: 10.1016/j.ins.2014.07.018
4. Dehmer M, Emmert-Streib F, Shi Y. Interrelations of graph distance measures based on topological indices. PLoS ONE. 2014; 9.
5. Cao S, Dehmer M, Shi Y. Extremality of degree-based graph entropies. Information Sciences. 2014; 278:22–33. doi: 10.1016/j.ins.2014.03.133
6. Gupta MK, Niyogi R, Misra M. A 2D Graphical Representation of Protein Sequence and Their Similarity Analysis with Probabilistic Method. MATCH Communications in Mathematical and in Computer Chemistry. 2014; 72:519–532.

7. Amidor I. Scattered data interpolation methods for electronic imaging systems:survey. Journal of Electronic Imaging. 2002; 11(2):157–176. doi: 10.1117/1.1455013
8. Dougherty RL, Edelman Z, Hyman JM. Non-negativity, monotonicity or convexity preserving cubic and quintic Hermite interpolation. Mathematics of Computation. 1989; 52(186):471–494. doi: 10.1090/S0025-5718-1989-0962209-1
9. Piah ARM, Goodman TNT, Unsworth K. Positivity preserving scattered data interpolation. In: Martin R, Bez H, Sabin M, editors. Proceeding of Mathematics of Surfaces, Lecture Notes in Computer Science,3604. New York: Springer-Verlag Berlin Heidelberg; 2005. p. 336–349.
10. Hussain MZ, Hussain M. Shape preserving scattered data interpolation. European Journal of Scientific Research. 2009; 25(1):151–164.
11. Hermann M, Mulansky B, Schmidt JW. Scattered data interpolation subject to piecewise quadratic range restriction. Journal of Computational and Applied Mathematics. 1996; 73:209–223. doi: 10.1016/0377-0427(96)00044-1
12. Hussain MZ, Hussain M. C^1 positivity preserving scattered dat interpolation using Bernstein Bezier triangular patch. Journal of Applied Mathematics and Computing. 2011; 35:281–293. doi: 10.1007/s12190-009-0356-0
13. Ibraheem F, Hussain M, Hussain MZ, Bhatti AA. Data visualizaation using Trigonometric function. Journal of Applied Mathematics. 2012; 2012:1–19. doi: 10.1155/2012/247120
14. Nielson GM. The side-vertex method for interpolation in triangles. Journal of Approximatio Theory. 1979; 25:316–336.
15. Goodman TNT, Said HB, Chang LHT. Local derivative estimation for scattered data interpolation. Applied Mathematics and Computation. 1995; 68:41–50. doi: 10.1016/0096-3003(94)00086-J
16. Davidson KR. The Evolution of Cooperation. Newyork: Basic Books; 2006.
17. Ma ZQ, Xia CY, Sun SW, Wang L, Wang HB, Wang J. Heterogeneous link weight promotes the cooperation in spatial prisoner's dilemma. International Journal of Modern Physics C. 2011; 22:1257–1258. doi: 10.1142/S0129183111016877
18. Jaun W, Yi XC, Yiling W, Shuai D, JunQing S. Spatial prisoner's delimma games with increasing size of the interaction neighborhood on regular lattices. Chinese Science Bulletin. 2012; 57:724–728. doi: 10.1007/s11434-011-4890-4